

2009 年度 財団法人交流協会フェローシップ事業成果報告書

SLOPE TOPOGRAPHY MEASUREMENT USING
PHOTOGRAPHIC TECHNICS WITHOUT TARGETS

国立成功大学

吳建宏

招聘期間(2009年8月2日～9月12日)

2009年12月

財団法人 交流協会

SLOPE TOPOGRAPHY MEASUREMENT USING PHOTOGRAPHIC TECHNICS WITHOUT TARGETS

Jian-Hong WU

Department of Civil Engineering, National Cheng Kung University, Tainan, Taiwan

INTRODUCTION

Taiwan is located at the boundary of Eurasian and Phillipines sea plates. Large tectonic force causes frequent earthquakes, complicated geologic structures, fractured rock mass, and craggy landform. Roughly 70% of the area on this island is hills and mountains. In addition, earthquakes, typhoons, and heavy rainfalls are vital external forces that usually cause slope failures to result in casualties and loss of properties on this island. Severe slope failures occurred during the Chi-Chi earthquake, Mindulle and Aere typhoons are unforgettable disasters in Taiwan (ITRI, 2004). Although similar geological and geotectonic background exists in Japan, introducing new concepts and technologies to mitigate the damage caused by landslides are crucial tasks for the engineers of both countries.

A large landslide significantly changes local landform although aerial photos with topographic contour before the landslide occurred. In the cases of Chiu-fen-erh-shan (Fig. 1) (Wu et al., 2005; Wu, 2007; Wu et al., 2009) and Tsaoling landslides (Fig. 2) (Chigira et al., 2003) happened in Chi-Chi earthquake and the Tuchang landslide happened during the Aere typhoon as shown in Fig. 3, the large landslides caused numerous and serious damages to the local residents. In August of 2009, typhoon Morakot brought more than 2000 mm rainfalls to southern Taiwan in three days and collapsed the slope to bury more than 300 local residents in Shiaolin village at Kaohsiung County. Updated topography after the landslides or determining the size of the unstable area is very useful in

evaluating the volume of debris, designing the countermeasures, and the landslide analysis. However, obtaining the real-time three-dimensional landform is still a difficult task in disaster prevention.



Fig. 1 Chiufenerhshan Landslide



Fig. 2 Tsaoling Landslide



Fig. 3 Tuchang Landslide

Surveyors may in danger because they must put the measuring targets at the unstable slope when conducting conventional survey. In addition, the survey causes a long time if the landslide is large. A laser scanning technique called Lidar and the conventional aerial photo are alternative technologies that enable us to generate the topographic contours of the slope after a landslide. Lidar is safer than

the conventional survey because they measure the landform away from the landslide. In addition, shorter time for the survey is needed because the device measures several points on the objective body simultaneously. However, the high cost of the equipments and the requirement of renting an airplane usually delay the time to obtain the three-dimensional landform data. Therefore, the satellite image and aerial photo are expected as a base to obtained real-time three-dimensional landform because they easily enable engineers to take a look at the “outlook” of a landslide. The current problems of using satellite image and aerial photo to obtain the landform of a slope are listed below:

1. Special calibrated camera is required when using aerial photo to obtain the slope landform. The cost of the special camera is very high.
2. The airplane is required to take aerial photo and no picture will be available when the airplane is not allowed to go.
3. Satellite image is another approach to obtain three-dimensional slope landform, however, the resolution is lower than aerial photo, and new technique is required to interpret the data.

On the other hand, digital vision metrology is a calculation algorithm in obtaining the coordinates of targets through the pictures taken by digital camera and has the advantage of obtaining the three-dimensional coordinates of many measurement points at cheap cost. Ryu et al. (2005) validated the applicability of using digital vision metrology to monitor an unstable slope. Therefore, the basic concepts of digital metrology and their experiences are expected to be learned when visiting Kyoto University since the new technology was developed by its researchers. However, measuring targets are necessary so far. Attaching targets on an unstable slope is a dangerous task and the resolution of satellite images is too low to have common targets on the slope. Thus, we attempt to evaluate the non-target algorithm and incorporate digital vision metrology to obtain real-time landform data using satellite in the future. Up-to-date, increasing the accuracy of non-target digital vision metrology

remains a difficult task and needs further studies because identifying the same point from different pictures is difficult. The research results are expected to improve the digital vision metrology but also provide alternative method to obtain real-time three-dimensional landform.

THEORY OF DIGITAL VISION TECHNOLOGY

Collinearity formula in conventional photogrammetry is the transferring formula to get the three-dimensional coordinates of a point from the two-dimensional coordinates on an image. In other words, targets are attached to the measured object, numerous images of targets are taken from different locations in different photograph angles. Specified target is identified from tens of images on the computer screen. Three-dimensional coordinates of the targets are back calculated from the two-dimensional coordinates on the images.

Despite of obtaining the two-dimensional centroid coordinates of each target on the image, lens distortion, CCD distortion, and distortion of width/length ratio are parameters that must be solved in the computation algorithm.

Fig. 1 shows the geometrical relations between a measurement point, the camera and the image of measurement point. The image plane demonstrates a film of the camera. A digital camera uses electric sensing devices in the location of the conventional film. The devices are mounted in the focal plane of a camera, thus the two-dimensional coordinates $p(x, y)$ of each target in every image are known. The three-dimensional coordinates of the target $P(X, Y, Z)$, the location of photographing $O(X_O, Y_O, Z_O)$, and the orientation of the camera (θ, ϕ, κ) are unknown parameters. The collinearity formula derived by the geometry of target (P), center of lens (O), and target image (p) is shown as Eq. (1). The $(x, y, -c)$ in Eq. (1) shows the two-dimensional coordinates of the target image (p) in camera coordinate system with focal length c . The parameters $(\Delta x, \Delta y)$ come from the eight deviators of the image (Weng et al., 1992). (X_O, Y_O, Z_O) are the center of lens. (X, Y, Z) are the

three-dimensional coordinates of the target in space coordinate system. The m_{ij} is the transfer matrix between space coordinate system and camera coordinate system.

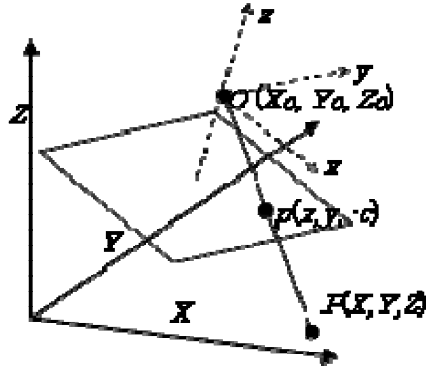


Fig. 1 Geometry of collinearity in digital photography

$$x = \Delta x - c \frac{m_{11}(X - X_o) + m_{12}(Y - Y_o) + m_{13}(Z - Z_o)}{m_{31}(X - X_o) + m_{32}(Y - Y_o) + m_{33}(Z - Z_o)} \quad (1a)$$

$$y = \Delta y - c \frac{m_{21}(X - X_o) + m_{22}(Y - Y_o) + m_{23}(Z - Z_o)}{m_{31}(X - X_o) + m_{32}(Y - Y_o) + m_{33}(Z - Z_o)} \quad (1b)$$

1. Rotation Matrix of the Camera

The m_{ij} in the collinearity formula is defined to be the rotation matrix of the camera, as also the transformation matrix of the camera attitude. Initial values must be involved to the linear extension of Eq. (1). Therefore, methods regarding to the photographing direction must be considered. The simply overlapping of the origin must be done for the parallel translation is occurred in two different coordinate systems. Fig. 2 illustrates rotational mapping between two coordinate systems:

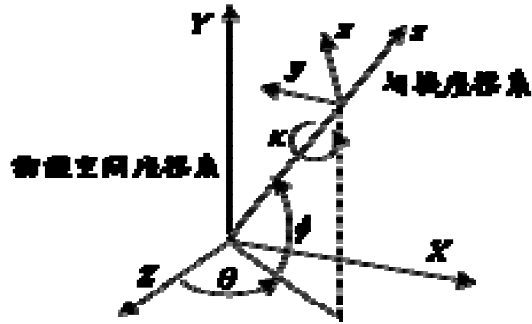


Fig. 2 Rotational mapping between two coordinate systems

- 1) Y is defined to be the axis of the horizontal rotation. When we face to the axis, rotation to the right is defined to be positive. The θ is called azimuth.
- 2) X is defined to be the axis of the vertical rotation. Rotating upward indicates the positive vertical rotation. The angle of φ is defined to be elevation.
- 3) Z is a rotating axis that the positive indicates rotating counter-clockwise. The angle κ is defined to be rolling.

The angle definition is similar to the Total Station apparatus. However, the vertical axis is defined to be 0 in total station; while the photogrammetry defines 0 in horizon. In addition, the Total Station defines Z-axis as positive; while, the photogrammetry defines positive as Y-axis.

The rotational matrices of above-mentioned 1), 2), and 3) are defined to be m_θ , m_φ , and m_κ . Each matrix can be calculated as the following Eq. (2):

$$m_\theta = \begin{bmatrix} \cos \theta & 0 & \sin \theta \\ 0 & 1 & 0 \\ -\sin \theta & 0 & \cos \theta \end{bmatrix} \quad (2a)$$

$$m_\phi = \begin{bmatrix} 1 & 0 & 0 \\ 0 & \cos \phi & -\sin \phi \\ 0 & \sin \phi & \cos \phi \end{bmatrix} \quad (2b)$$

$$m_\kappa = \begin{bmatrix} \cos \kappa & \sin \kappa & 0 \\ -\sin \kappa & \cos \kappa & 0 \\ 0 & 0 & 1 \end{bmatrix} \quad (2c)$$

Equation (3) indicates the multiplications of Eq. (2) to get the rotational matrix, M. In other words, the nine items of m_{ij} in the collinearity formula (Eq. (1)) is defined by Eq. (3). The θ , ϕ , and κ are independent varies regarding to the attitude of camera for photographing.

$$M = m_\kappa m_\phi m_\theta = \begin{pmatrix} m_{11} & m_{12} & m_{13} \\ m_{21} & m_{22} & m_{23} \\ m_{31} & m_{32} & m_{33} \end{pmatrix} \quad (3a)$$

$$\left. \begin{aligned} m_{11} &= \cos \kappa \cos \theta - \sin \kappa \sin \phi \sin \theta \\ m_{12} &= \sin \kappa \cos \phi \\ m_{13} &= -\cos \kappa \sin \theta - \sin \kappa \sin \phi \cos \theta \\ m_{21} &= -\sin \kappa \cos \theta - \cos \kappa \sin \phi \sin \theta \\ m_{22} &= \cos \kappa \cos \phi \\ m_{23} &= \sin \kappa \sin \theta - \cos \kappa \sin \phi \cos \theta \\ m_{31} &= \cos \phi \sin \theta \\ m_{32} &= \sin \phi \\ m_{33} &= \cos \phi \cos \theta \end{aligned} \right\} \quad (3b)$$

2. Calculating the centroid of the target

The gray scale distribution technique is used to calculate the two-dimensional centroid coordinate of each target taken in the picture. The threshold of the gray scale can be automatically set and the

pixels below the threshold of the gray scale are considered to be noise, and the gray scales are set to be 0. In Eq. (4), the gray scale of each pixel is concerned to be the weighting of the pixel. The (x, y) are the centroid of the pixel. (x_0, y_0) are the origin of the coordinate. (a_x, a_y) are the size of the pixel. $q(i,j)$ are the gray scale of the pixel at (i, j) . The accuracy of the calculations is strongly governed by the number of the pixel with target to the total number of pixels. The accuracy can be up to 1/10 of the pixel size.

$$\begin{aligned}
 x &= x_o + a_x \cdot \frac{\sum_{i=1}^n \sum_{j=1}^m (q(i,j) \times x_{ij})}{\sum_{i=1}^n \sum_{j=1}^m q(i,j)} \\
 y &= y_o + a_y \cdot \frac{\sum_{i=1}^n \sum_{j=1}^m (q(i,j) \times y_{ij})}{\sum_{i=1}^n \sum_{j=1}^m q(i,j)}
 \end{aligned} \tag{4}$$

When applying digital photogrammetry technique to measure the slope deformation, tens to hundreds of targets must be defined from tens of pictures. Therefore, the initial coordinates of the measuring points, the attitude of the camera, and the numbering and the exact two-dimensional coordinate of each target in the pictures must be achieved nearly real-time to have practical value.

UNINHABITED AERIAL VEHICLES (UAV)

Despite of the developments of digital photogrammetry, the uninhabited aerial vehicles (UAV) is another key development to obtain 3D topography during a disaster. Before visiting Japan, we assume that the satellite image is a very useful tool to get 3D topography. However, Typhoon Morakt seriously damaged the mountainous areas of the southwestern Taiwan and even destroyed the

Shiaolin village in Kaohsiung County. We suddenly reminded that the satellite image has limitation on cloudy weather. Additional platform must be considered to improve the situation, and the UAV seems to be an alternative solution to have local pictures, even the weather is cloudy.

Yugas (2006) mentioned that the development of military UAV is shown in Fig. 3. In addition, he also mentioned that UAV can be used to measure gradual movement of hillsides as a result of heavy rainfalls may eventually lead to catastrophic landslides. Accurate measurements of surface deformation over areas prone to landslide will assist in assessment of the process. Therefore, the UAV is expected to be a platform that has lower flight altitude and cost to have high-resolution pictures than the satellite image.

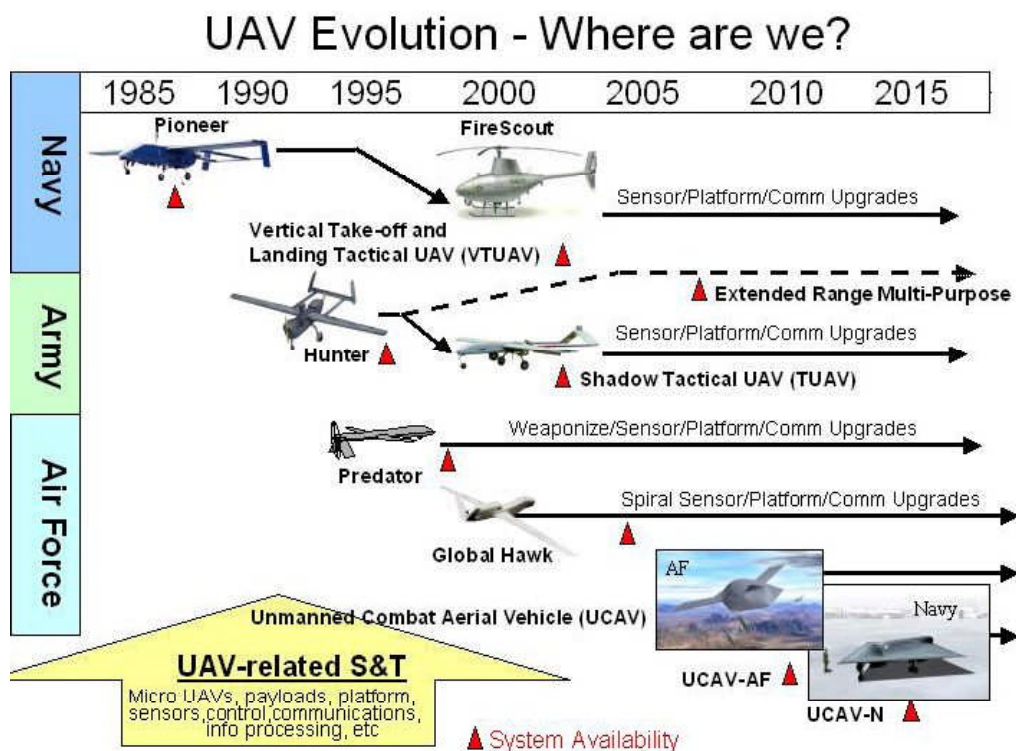


Fig. 3 Development of military UAV

Certainly, we can apply the same photography techniques to the pictures taken by the UAV to have the topographic data.

IMAGE METHOD

Barton and Choubey (1977) proposed the ten standard joint profiles for the Joint Roughness Coefficient (JRC) as an index for the joint roughness. Hsieh (2002) proposed a new technique to evaluate the shear strength of artificial joint surface using image method. In his technique, a new device (Fig. 5) was developed to measure the joint images. Figure 6 illustrates that the new device for the joint image have better resolutions than the joint images taken by the camera. Since the light and the shadow of the picture indicate different topographic pattern on the sample, we expected that this technique can be improved to have 3D topographic data in the future.

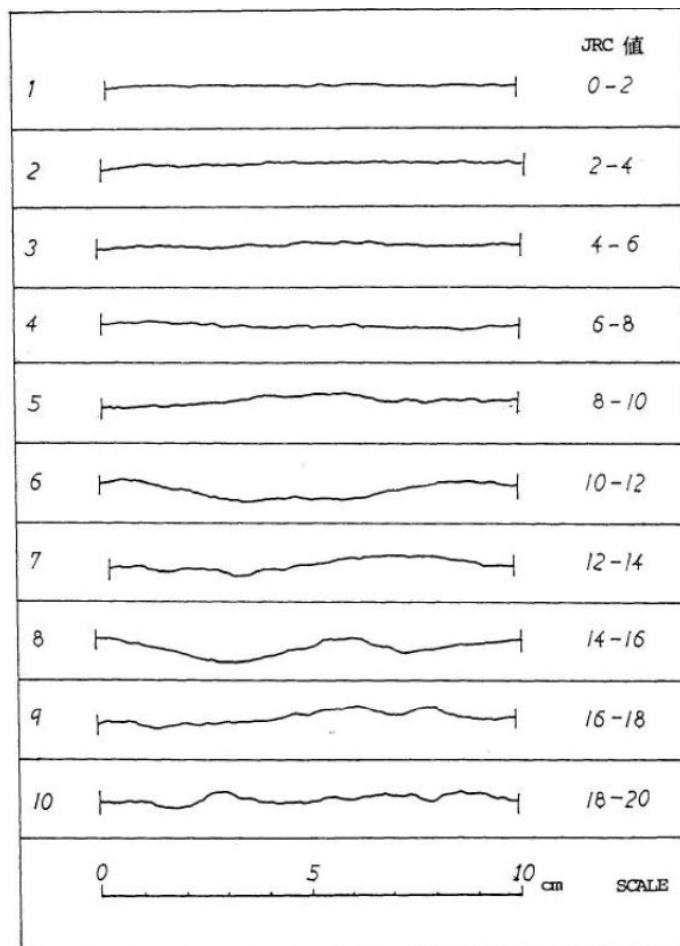


Fig. 4 Ten standard joint profiles (Barton and Choubey, 1977)

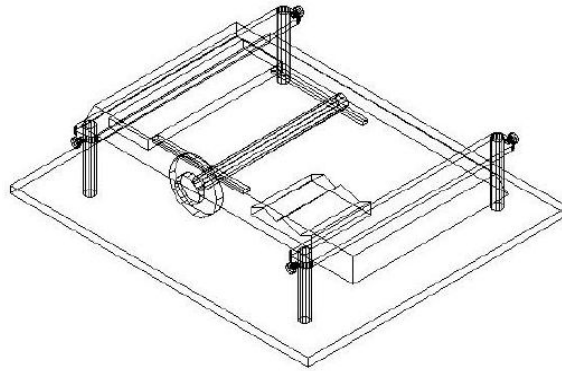


Fig. 5 New device for the joint image (Hsieh, 2002)

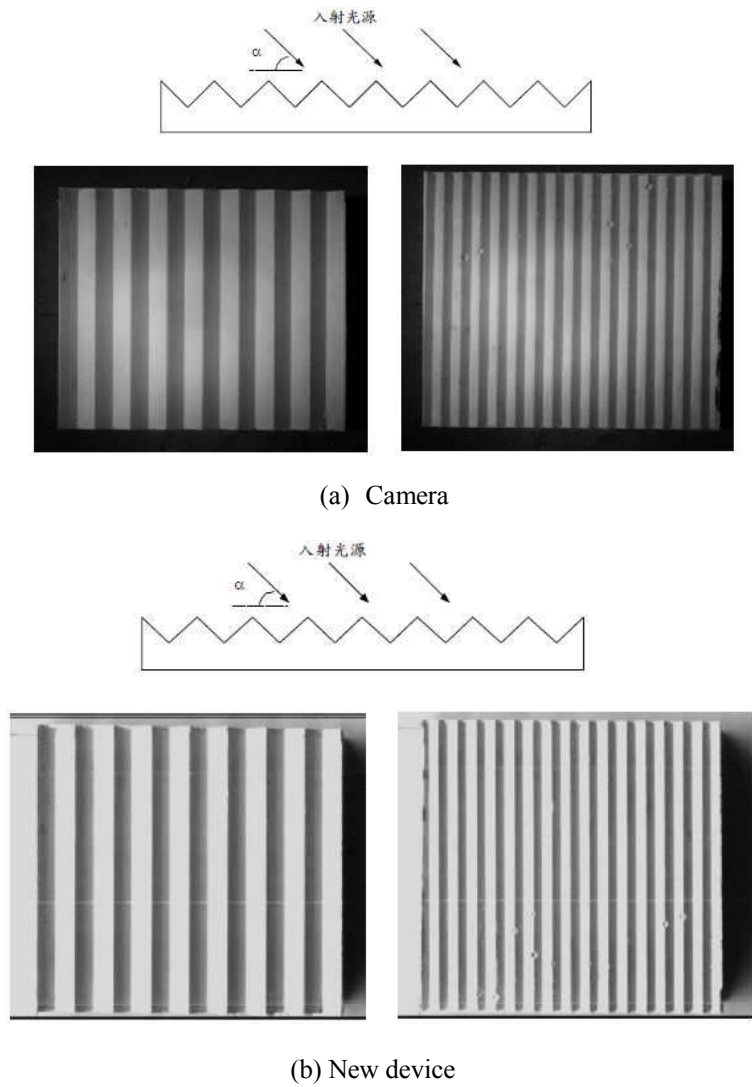


Fig. 6 Joints taken by camera and new device for the joint image (Hsieh, 2002)

RADIO PHASE DISPLACEMENT MEASUREMENT METHOD

The basic concept of the radio phase displacement measurement system for long time measurement is shown as Fig. 7. In this system, radio transmitters are attached on multiple measurement point in landslide area. Passive sensors are set on static points in steady area. Each transmitter of measurement point transmits the radio wave with very small frequency difference from other transmitters to isolate the transmitters.

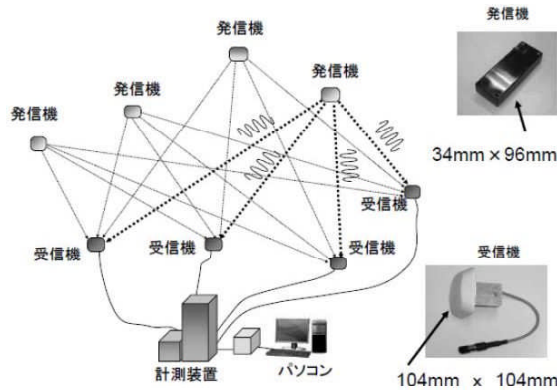


Fig. 7 Radio phase displacement measurement devices

When processing the signal, received signals are digitized by A/D converters. The digital received signals of sensors are turned to the frequency domain, and the transmitted signal frequency is obtained. The phase angle of the obtained frequency is calculated and demonstrates the propagation length between transmitters and receivers. A phase angle of the i th transmitter to the j th receiver can be written as follows:

$$\phi_{ij} = \frac{2\pi}{\lambda} \sqrt{(x_i - X_j)^2 + (y_i - Y_j)^2 + (z_i - Z_j)^2} + \psi_i + \xi_j + 2\pi N_{ij} \quad (5)$$

Where, λ is the radio wave length. (X_j, Y_j, Z_j) is the position of the receiver. (x_i, y_i, z_i) is the

position of transmitter. ψ_i is the phase angle of transmitted signal at transmitter. ξ_j indicates the phase angle caused by the receiver channel delay. N_{ij} is the integer bias.

CONCLUSIONS

As the recent development of monitoring techniques, except the conventional photography technique with targets installed on the object to be measured, several new technologies are going on their way. The uninhabited aerial vehicles provide additional platform to carry out camera or Light Detection And Ranging (Lidar). In addition, the new image method proposed by Hsieh (2002) provides additional technology to investigate the topography through shadow and light. In his study, the images of different topography patterns correlate well with the JRC. However, further investigations are needed to use the technology to demonstrate the 3D landform in the future.

Furthermore, instead of the target used for photography technique, Japanese engineers develop radio phase displacement measurement devices, which are also known as “Inverse GPS system”. Different from the GPS that the satellite emits signals and the locations of the monitored receivers are calculated, the measured “target” in the radio phase displacement measurement device emits radio signals and the receiver is located out of the landslide area.

The mountainous areas in the southwestern Taiwan provide a very good study site for the new monitoring technologies, especially after the Typhoon Morakt. However, advanced studies are still required to generate a simple, cheap but real-time 3D topography.

References

- (1) N. Barton, V. Choubey, 1977, “The Shear Strength of Rock Joints in Theory and Practice”, Rock Mechanics, Vol. 10, pp. 1-54.
- (2) M. Chigira, W.N. Wang, T. Furuya, T. Kamai, 2003, “Geological Causes and Geomorphological

- Precursors of the Tsaoling Landslide Triggered by the 1999 Chi-Chi Earthquake, Taiwan,”
Engineering Geology, Vol. 68, No. 3-4, pp. 259-273.
- (3) M.-C. Hsieh, 2002, “Research of Image Method Applied on The Shear Strength of Artificial Joint Surface”, Master Thesis, Department of Civil Engineering, National Cheng Kung University, Tainan, Taiwan.
- (4) ITRI, 2004, “Disaster Investigations and Their Recovery Policies Cause by Aere Typhoon,” Council for Economic Planning and Development, Taipei, Taiwan (in Chinese)
- (5) M. Ryu, T. Nakai, Y. Ohnishi, S. Nishiyama, T. Yano, DH Lee, SK Chang, 2005, “Applying Digital Vision Metrology to Slope Monitoring,” Taiwan-Japan Joint Underground Investigations and Detecting Techniques Forum, Taipei, Taiwan, pp. 105-110.
- (6) N. Sasaki, T. Amishima, A. Okamura, W. Yoshizaki, K. Nishikawa, Y. Ohnishi, S. Nishiyama, T. Yano, D-H. Lee, J-H Wu, 2005, “Radio Phase Displacement Measurement Method for Disaster Prevention and Monitoring”, Taiwan-Japan Joint Conference on Underground Space Investigation and Monitoring Technologies, Taipei, Taiwan, pp. 117-123.
- (7) J. Weng, P. Cohen, and M. Herniou, 1992, “Camera Calibration with Distortion Models and Accuracy Evaluation,” IEEE Transaction on Pattern Analysis and Machine Intelligence, Vol.14, No.10, pp.965-980.
- (8) J.H. Wu, W.N. Wang, C.S. Chang and C.L. Wang, 2005, “Effects of Strength Properties of Discontinuities on the Unstable Lower Slope in the Chiu-fen-erh-shan Landslide, Taiwan,” Engineering Geology, Vol. 78, pp.173-186.
- (9) J.H. Wu, 2007, “Applying Discontinuous Deformation Analysis to Assess the Constrained Area of the Unstable Chiu-fen-erh-shan Landslide Slope,” International Journal for Numerical and Analytical Methods in Geomechanics, Vol. 31, Issue 5, pp. 649-666.
- (10) J.H. Wu, J.S. Lin, and C.S. Chen, 2009, “Dynamic Discrete Analysis of an Earthquake-Induced

Large Scale Landslide,” International Journal of Rock Mechanics and Mining Sciences, Vol. 46,
Issue 2, pp. 397-407.

(11)C. Yuhas, 2006, “Earth Observations and the Role of UAVs: A Capabilities Assessment”

(http://ntrs.nasa.gov/archive/nasa/casi.ntrs.nasa.gov/20070022505_2007021261.pdf)